



Effect of surface coating and organic matter on the uptake of CeO₂ NPs by corn plants grown in soil: Insight into the uptake mechanism

Lijuan Zhao^a, Jose R. Peralta-Videa^a, Armando Varela-Ramirez^c, Hiram Castillo-Michel^d, Chunqiang Li^e, Jianying Zhang^c, Renato J. Aguilera^c, Arturo A. Keller^f, Jorge L. Gardea-Torresdey^{a,b,*}

^a Chemistry Department, The University of Texas at El Paso, 500 West Univ. Av., El Paso, TX 79968, United States

^b Environmental Science and Engineering PhD program, The University of Texas at El Paso, 500 West Univ. Av., El Paso, TX 79968, United States

^c Department of Biological Sciences, Border Biomedical Research Center, The University of Texas at El Paso, 500 West Univ. Av., El Paso, TX 79968, United States

^d European Synchrotron Radiation Facility, B.P.220 – 38043 Grenoble Cedex, France

^e Physics Department, The University of Texas at El Paso, 500 West Univ. Av., El Paso, TX 79968, United States

^f Bren School of Environmental Science & Management, UC Center for the Environmental Implications of Nanotechnology, 3420 Bren Hall, University of California, Santa Barbara, CA 93106, United States

H I G H L I G H T S

- First report on the effects of surface coating on Ce uptake from CeO₂ NPs by corn plants.
- First report upon the mechanisms of CeO₂ NPs uptake by corn plants.
- First report on the effects of organic matter on Ce/CeO₂ NPs uptake by corn plants.

A R T I C L E I N F O

Article history:

Received 2 February 2012

Received in revised form 27 April 2012

Accepted 1 May 2012

Available online 9 May 2012

Keywords:

CeO₂ NPs
Root uptake
Translocation
Fluorescence
Zea mays

A B S T R A C T

Little is known about the fate, transport, and bioavailability of CeO₂ nanoparticles (NPs) in soil. Moreover, there are no reports on the effect of surface coating upon NPs uptake by plants. In this study, *Zea mays* plants were grown for one month in unenriched and organic soils treated with coated and uncoated CeO₂ NPs. In addition, plants were exposed to fluorescein isothiocyanate (FITC)-stained CeO₂ NPs and analyzed in a confocal microscope. In organic soil, roots from uncoated and coated NPs at 100, 200, 400, and 800 mg kg⁻¹ had 40, 80, 130, and 260% and 10, 70, 90, and 40% more Ce, respectively, compared to roots from unenriched soil. Conversely, shoots of plants from unenriched soil had significantly more Ce compared with shoots from organic soil. Confocal fluorescence images showed FITC-stained CeO₂ NP aggregates in cell walls of epidermis and cortex, suggesting apoplastic pathway. The μ XRF results revealed the presence of CeO₂ NP aggregates within vascular tissues. To the authors knowledge this is the first report on the effects of surface coating and organic matter on Ce uptake from CeO₂ NPs and upon the mechanisms of CeO₂ NPs uptake by higher plants.

© 2012 Elsevier B.V. All rights reserved.

1. Introduction

Cerium oxide (CeO₂) NPs are widely used as polishing materials, additive in glass and ceramic, fuel cell materials, in agricultural products, and automotive industry [1–3]. In automotive industry, these NPs are used in emission control systems to reduce particulate matter emissions [4]. As a result, substantial amounts of CeO₂ NPs are directly released into either the troposphere or the soil.

Nanoparticles released into the air will precipitate with the rain and deposited in the soil. Limbach et al. [5] estimated that CeO₂ NP concentrations would be varying between 0.32 and 1.12 mg kg⁻¹ levels depending on the soil depth and the distance from highways. This suggests that CeO₂ NPs will consistently increase in the environment. However, the knowledge regarding their environmental fate and behavior is still scarce [4,6].

Previous studies investigated the transport and deposition of CeO₂ NPs in water-saturated columns packed with sand and the role of the water chemistry was also investigated [6]. Cornelis et al. for the first time investigated the solubility and retention of CeO₂ nanoparticles in real soil system [7]. These researchers reported that the dissolution of CeO₂ NPs in soil solutions at pH 4 was less than 3.1%, but no dissolution was detected at pH values of 7 and

* Corresponding author at: Chemistry Department, The University of Texas at El Paso, 500 West Univ. Av., El Paso, TX 79968, United States. Tel.: +1 915 747 5359; fax: +1 915 747 5748.

E-mail address: jgardea@utep.edu (J.L. Gardea-Torresdey).

9 [7]. Concerning the interaction of CeO₂ NPs with living organisms, reports indicate that these NPs can be taken up and generate toxicity in algae, zebrafish, and human lung fibroblast cells [8–11]. However, there is limited work on plant uptake, and most of the reported studies were performed in hydroponics [12–14]. Terrestrial plants, especially crops, play an important role in the transport of soil constituents to primary consumers [15–17]. Therefore, it is imperative to investigate the behavior of CeO₂ NPs in soil and the uptake rate by plants grown in CeO₂ NP impacted soil. Undoubtedly, this information will contribute to determine if these NPs can be put in the food chain threatening the ecosystems and human health.

In a recent report, X-ray absorption near-edge structure (XANES) showed clear evidence that corn plants grown in hydroponics take up CeO₂ NPs through the roots without modification [12]. However, there are very few reports on the uptake of CeO₂ NPs by corn plants from real soil systems [14]. Corn is one of the three most important food crops worldwide. It is consumed directly in Latin America and indirectly as feed for livestock in other countries [18]. Due to the interactions between NPs and soil (chemical attachment with organic matter and clay minerals and physical straining), the mobile and bioavailable fraction of NPs in soil solution will be much lower compared to hydroponic solutions. Results from hydroponic experiments may be differed from real systems.

Very often, the stability of NPs is improved by surface coating. In such circumstances, the interaction of the coated NPs with soil may be altered. NPs have high surface reactivity and coatings may increase their adhesion to reactive soil surfaces and may enhance their transport [19]. Parsons et al. reported that citrate coating increased the absorption and biotransformation trend of Ni(OH)₂ NPs fed to hydroponically grown mesquite plants [20]. Citrate was considered responsible for the increased uptake in that study. However, no reports were found about the effect of surface coating on the CeO₂ NP behavior in soil.

Depth studies on the localization of NPs in plant tissues are needed in order to better understand their behavior in plants [16]. By using TEM images ZnO NPs were observed penetrating the endodermal and vascular cells of ryegrass roots [21]. In addition, by using conventional light microscopy and taking advantage of the black color of bioferrofluid, the distribution of magnetic carbon-coated NPs in different plants was studied [22]. They found that the NPs easily penetrated the root, reached the vascular cylinder and moved in the xylem vessels to the aerial part of the plants using the transpiration stream. Using two-photon excitation microscopy coupled with autofluorescence technique, Wild and Jones [23] have shown that multiwalled carbon nanotubes (MWCNTs) primarily adsorbed to root surface as individual and aggregated CNTs. Dye staining is a potential observation method for non-fluorescence emission NPs. Images from confocal microscopy distinctly demonstrated that fluorescein isothiocyanate (FITC)-stained metal oxides NPs were taken up by human cells [24]. Other researchers used the same technique to show that FITC-stained single-walled carbon nanotubes (SWNTs) successfully penetrated the wall of cultured plant cells [25]. However, no reports were found on the use of FITC-staining technique to study the uptake of metal oxide NPs by a whole plant.

In the present study, the uptake of CeO₂ NPs by corn plants grown in soil was investigated. The effect of surface coating and soil organic matter on the uptake and accumulation of CeO₂ NPs by corn plants were also determined. Corn kernels were sown in a natural sandy loamy soil and a mixture of the sandy loamy soil plus potting soil with high organic matter content. In addition, to clarify the uptake and transport pathway within the plants, three week-old corn plants were allowed to grow in a FITC-CeO₂ NPs suspension, cryo-sectioned and imaged in a confocal microscope. Samples were also analyzed using micro X-ray fluorescence (μ XRF) and micro

X-ray absorption near edge structure (μ XANES). Ce concentrations in soil and plants were determined by using inductively coupled plasma-optical emission/mass spectrometry (ICP-OES) and (ICP-MS).

2. Materials and methods

2.1. Soil and NPs preparation

The soil for these studies was collected from Horizon, TX (31°51'59.06"N; Elev. 1144 m, top 20 cm), air-dried and sieved through a 1 mm mesh prior to experimental use. The soil was classified as sandy loam soil (unenriched soil). Because the Horizon soil has very low organic matter content, a portion of this soil was mixed 1:1 with a potting soil with high organic matter purchased from a nursery store (Scotts, premium potting soil). This was called organic soil. Other characteristics of both soils are described in Table S1.

Uncoated CeO₂ NPs (Meliorum Technologies, New York) were obtained from the University of California Center for Environmental Implications of Nanotechnology. Previous characterization indicated that the CeO₂ NPs had a primary size of 8 ± 1 nm, with a hydrodynamic size of 1373 ± 32 nm and zeta potential of $-0.62 (\pm 2.9)$ mV. Size and zeta potential of nanoparticle in suspensions were measured using a Malvern Zetasizer (Nano-ZS 90, Malvern). All the size and zeta potential determinations were performed in CeO₂ NP suspensions at 25 mg L^{-1} . When analyzing zeta potential, three measurements, consisting of 12 runs each, were acquired for each sample. SEM images are shown in Fig. S1.

The coating of CeO₂ NPs with alginate is done simply by dispersing the CeO₂ NPs in the alginate suspension at the desired concentrations. Following work by Keller et al. [26], as well as several other studies, it can be determined that the alginate attaches to the CeO₂ NPs by measuring the electrophoretic mobility, which becomes significantly negative, leading to increased electrostatic repulsion.

The NP staining was performed as described by Xia et al. [24]. Specifically, 8 mg of bare CeO₂ NPs were suspended in 5 ml of dimethylformamide (DMF). Subsequently, a 1 μ L aliquot of amino-propyltriethoxysilane (APTS) dissolved in 50 μ L DMF was added to the CeO₂ NPs suspension and stirred for 24 h. After removing the supernatant by centrifugation (2236 g, Fisher Scientific, Marathon 8 K), the modified NPs were resuspended in 1 ml of DMF, mixed with a solution of 2 mg of FITC in 1 ml of DMF, and stirred for 4 h. After thoroughly washing of labeled NPs with DMF, 20 ml of DI was added to the FITC-stained NPs. The process was continued until no fluorescence was detected in the supernatant.

2.2. Cerium in soil solution

The soil solution was extracted following the procedure described by Krishnamurti and Naidu [27] with small modifications. Briefly, triplicate aliquots of 40 g of distilled water were added to 5 g of soil to bring the soil to saturation. Subsequently, 4 mg CeO₂ NPs were added to the saturated soil solution and thoroughly shaken for 24 h. This represented NP concentration of 800 mg kg^{-1} soil, which was the highest concentration used in this study. Soil solutions were extracted by filtration under vacuum using medium porosity filter paper (particle retention: 5–10 μ m, Fisher Scientific). The pore size of the filter paper was large enough to permit NPs or aggregated NPs to pass through. Finally, the volume was adjusted to 100 ml. The pH of soil solutions was measured immediately after filtration. For the Ce determination, the soil solutions were digested (HNO₃:H₂O₂; 1:4) and analyzed by ICP-OES and (PerkinElmer Optima 4300 DV, Shelton, CT) and ICP-MS (PerkinElmer Elan DRC-II).

The size and zeta potential of bare and coated NPs in DI and soil solution were determined and data is shown in Table S2.

2.3. Corn growth in CeO₂ NP spiked soils

Magenta boxes were filled out in triplicate with 400 g of unenriched and organic soils and sown with six corn kernels (Golden variety, Del Norte Seed Company, El Paso, TX) to have enough biomass for all determinations. Triplicate CeO₂ NP suspensions were sonicated for 30 min and applied to the soil to have final concentrations of 100, 200, 400, and 800 mg NPs kg⁻¹ soil. To avoid interferences with the NPs, no additional fertilizer was added to the soils. Plants were grown for 30 days at room temperature and 16/8 h light/dark cycle. During 30 days cultivation, field capacity was maintained. At harvest, plants were thoroughly flushed with tap water followed by deionized water (DI). After washings, plants were oven dried at 60 °C for 24 h (Fisher Scientific, Isotemp Oven) and processed for Ce determination.

2.4. Cerium in plant tissues

Dried ground root and shoot samples were microwave digested with a mixture of HNO₃ (65%) and H₂O₂ (30%) in capped Teflon pressure digestion vessels at 165 °C for 35 min in a microwave oven (CEM Corporation Mathews, NC) and analyzed for Ce using ICP-OES and ICP-MS. ICP-MS was used to determine Ce in shoots samples. Certified Reference Material (Peach leaves, NIST 1547) was processed as samples and the recovery rate was 100.82 ± 0.48.

2.5. Confocal microscope observation

In order to track the NPs in root tissues, three-week-old control plants were treated with FITC-stained CeO₂ NPs suspension for 24 h. After that, the plants were taken out of solution and thoroughly washed with distilled water. Subsequently, root samples from the absorption region (root hair region) were sectioned at 10 μm using a Minotome plus cryostat (Triangle Biomedical Science, Durham, NC) and observed utilizing a LSM 700 confocal microscope (Zeiss, New York, NY), equipped with a 10× objective and assisted with ZEN 2009 software (Zeiss, New York, NY). Since the microscope system is equipped with monochromatic camera (black and white), computerized (ZEN 2009 software) pseudo-color was applied to the fluorescence channel to achieve colored images. The FITC was excited with an argon laser emitting at 488 nm. The FITC fluorescence was detected by the green channel which has a bandpass filter of 510–550 nm.

2.6. Micro XRF and μXANES data acquisition

For the μXRF and μXANES studies, corn root samples (cultivated in 100 mg kg⁻¹ CeO₂ NP suspensions for 24 h) were carefully washed and dissected 0.5 cm up from the root tip, frozen in liquid nitrogen, and embedded into Tissue Tek resin (Sakura Finetek, Torrance, CA). Embedded samples were axially sectioned at 30 μm thick and mounted onto ultralene window film. Sections were lyophilized immediately after at -53 °C and 0.140 mbar pressure for 48 h (Labcono FreeZone 4.5, Kansas City, MO). Micro-XRF mapping of the distribution of Ce in roots was performed with incident energy at 5.8 keV during the continuous mode at beamline ID21 of the European Synchrotron Radiation Facility (ESRF, Grenoble France) [28]. The storage ring current during data acquisition ranged between 180 and 200 mA (continuous) operating at 6.0 GeV. The beam was focused with the use of a Fresnel zone plate to a size of 0.2 × 0.8 μm² (V × H) and the fluorescence signal was detected with a Si drift detector in vacuum. Two photodiodes were used to measure the incident and transmitted beam intensities. Dwell time

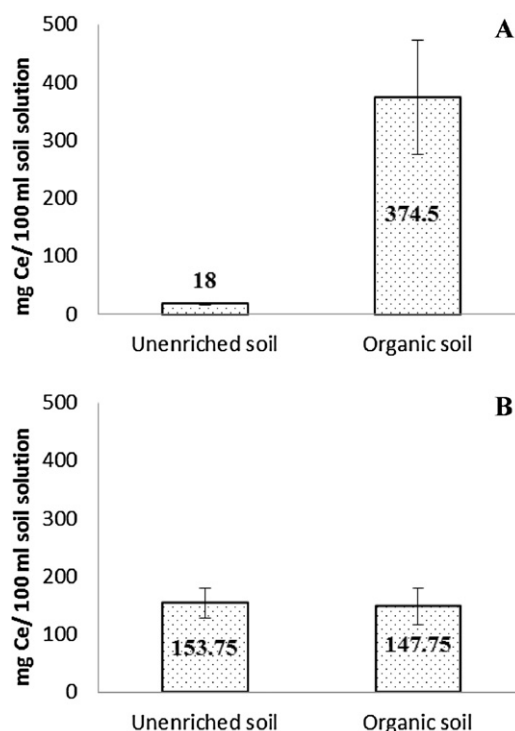


Fig. 1. Cerium concentrations in solutions of unenriched soil and organic soil treated with (A) uncoated CeO₂ NPs, and (B) coated CeO₂ NPs. Error bars stand for standard deviation.

and distance of the detector was optimized for each image keeping the detector dead time below 15%. The X-ray fluorescence data was fitted using PyMCA software [29]. For μXANES data acquisition, the energy of the monochromator (Si 111) was scanned from 5.69 to 5.79 keV and the zone plate was translated in the beam axis in order to maintain the beam focus. The final Ce-L^{III} edge spectra were the sum of 10 individual scans with 0.5 eV resolution steps. μXANES data analysis was carried using the ATHENA software. The pre-edge background was subtracted and normalized using a linear pre-edge. All peaks were identified by least-square fitting of Gaussian profiles and one arctangent function [30].

2.7. Statistical analysis

Ce concentrations in soil solution, roots, and shoots are averages of three replicates. A one-way ANOVA test was performed followed by Tukey-HSD test performed using the statistical package SPSS Version 12.0 (SPSS, Chicago, IL). Statistical significance was based on probabilities of $p \leq 0.05$.

3. Results and discussion

3.1. Cerium in soil solution

The soil solution contains the mobile fraction of elements and compounds available for plant uptake. As can be seen from Fig. 1A, Ce concentration in soil solutions from uncoated CeO₂ NPs in organic soil was much higher compared with unenriched soil. However, Ce concentrations in soil solutions from coated CeO₂ NPs were very similar in both soils (Fig. 1B). In the organic soil (0.77% C, Table S1) organic acids, such as humic and fulvic acids, increase NP mobility by surface coating of functional group on NP aggregate surfaces [31–33]. On the other hand, in unenriched soil (0.04% C) heterogeneous surface charge of colloidal clay bound the NP

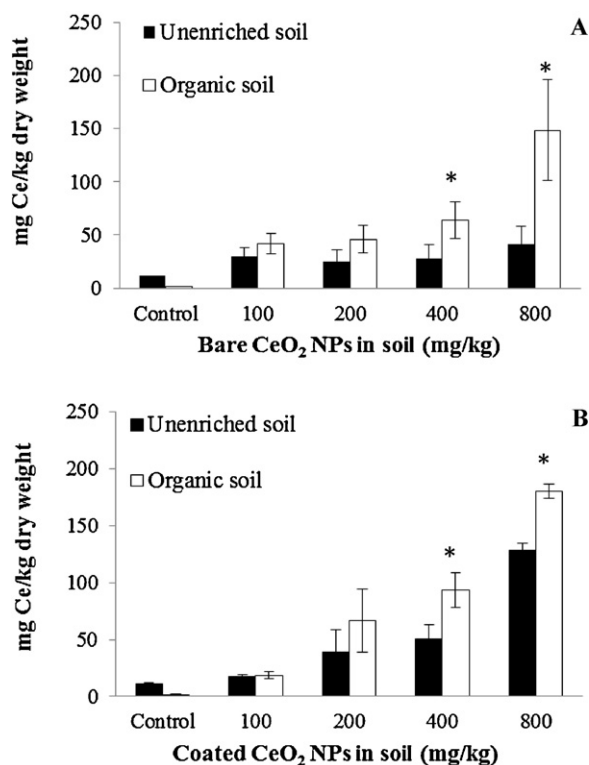


Fig. 2. Cerium concentrations in roots of corn plants (Golden variety) grown for one month in unenriched soil and organic soil treated with 0, 100, 200, 400, and 800 mg of CeO₂ NPs per kilogram soil (A) uncoated and (B) coated NPs. Error bars stand for standard deviation. * Stands for statistical differences between two soils at $\alpha < 0.05$.

aggregates and associated ions reducing their mobility to the soil solution [33].

By comparing Fig. 1A and B, it can be concluded that the mobility of CeO₂ NPs depends on the soil organic matter content, more than on the surface coating of the NPs. In unenriched soil surface, coated NPs have higher mobility than uncoated NPs. However, in organic soil surface coating decreased the NP mobility in soil solution.

3.2. Accumulation of Ce in corn roots

Concentrations of Ce in roots of corn plants grown in unenriched and organic soils and treated with coated and uncoated CeO₂ NP aggregates are shown in Fig. 2. As seen in this figure, the concentration of Ce in roots correlated well with the corresponding concentrations in soil for both coated and uncoated NPs, except coated NPs at 100 mg kg⁻¹. In addition, Fig. 2A and B shows that in all uncoated and coated NP treatments, higher amounts of Ce were found in roots of plants grown in organic soil. The increases were 40, 80, 130, and 260% for the treatments of 100, 200, 400, and 800 mg CeO₂ NPs kg⁻¹ soil, respectively. A previous report has shown that TiO₂, Al₂O₃, and ZnO NPs are bound to humic acid by electrostatic attraction and ligand exchange [32]. It is possible that the humic acid in organic soil increases the attachment of CeO₂ NPs to the root surface. In a very recent article Navarro et al. [34] reported that humic acids enhanced accumulation of CdSe/ZnS NPs onto the root surface of *Arabidopsis thaliana*. However, the mechanism is not clear and needs to be further studied.

The roots of plants grown in organic soil and treated with coated NPs had 10, 70, 90, and 40% more Ce compared to plants grown in unenriched soil (Fig. 2B). Although the presence of organic matter increased the amount of Ce in roots of plants treated with coated NPs, the increase was lower compared to uncoated NPs.

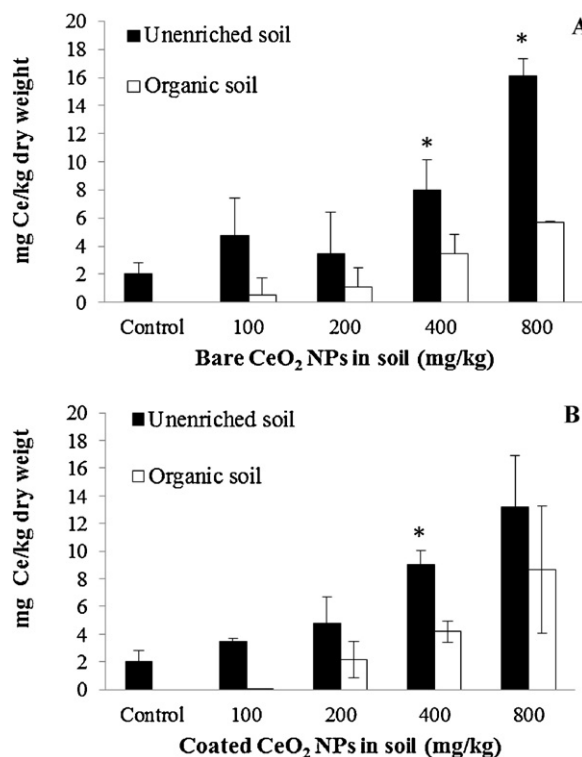


Fig. 3. Cerium concentrations in shoots of corn plants (Golden variety) grown for one month in unenriched soil and organic soil treated with 0, 100, 200, 400, and 800 mg CeO₂ NPs kilogram soil (A) uncoated and (B) coated NPs. Error bars stand for standard deviation. * Stands for statistical differences between two soils at $\alpha < 0.05$.

Carboxyl groups (–COOH) in the alginate solution, adsorbed by surface complexation onto the CeO₂ NPs, turned negative the surface charge of the NPs [31]. As shown in Table S2, the zeta potential of alginate acid coated NPs was respectively –93 and –92 for DI and soil solution. Thus, coated NPs could bind onto the acid-base behavior of colloidal soil clay with heterogeneous charge distribution [35]; which in turn reduced the availability of NPs for root uptake.

The results also showed that the surface coating plays an important role in the uptake of NPs by plants. As shown in Fig. S2, at 200 mg kg⁻¹ treatment and above, surface coating increased Ce accumulation in corn root tissues in both soils.

3.3. Translocation of Ce from roots to shoots

To investigate the translocation of Ce from roots to shoots, samples of plants grown with coated and uncoated Ce NPs were digested and analyzed using ICP-MS. Ce was detected in all shoots samples (Fig. 3). This finding differs from the results reported by Birbaum et al. [14], who exposed 3-week old maize plants for 14 days in soil irrigated with CeO₂ nanoparticle at 40.1 mg kg⁻¹. These researchers reported no Ce in stem and leaves and concluded that there was no Ce translocation from roots to shoots. In the present study, Ce was found at low concentrations in shoots of all plants, including control (~18–24 mg Ce kg⁻¹ soil, Table S1) grown in unenriched soil. However, Ce was not detected in control plants grown in organic soil and barely detected in plants treated with coated CeO₂ NPs at 100 mg kg⁻¹. This result coincides with the result reported by Birbaum et al. [14]. This suggests that the type of soil and NP surface charge could be responsible for the different response. The big difference in translocation factors (Ce in shoots/Ce in roots) between the two soils could support this hypothesis. The translocation factors of Ce in plants

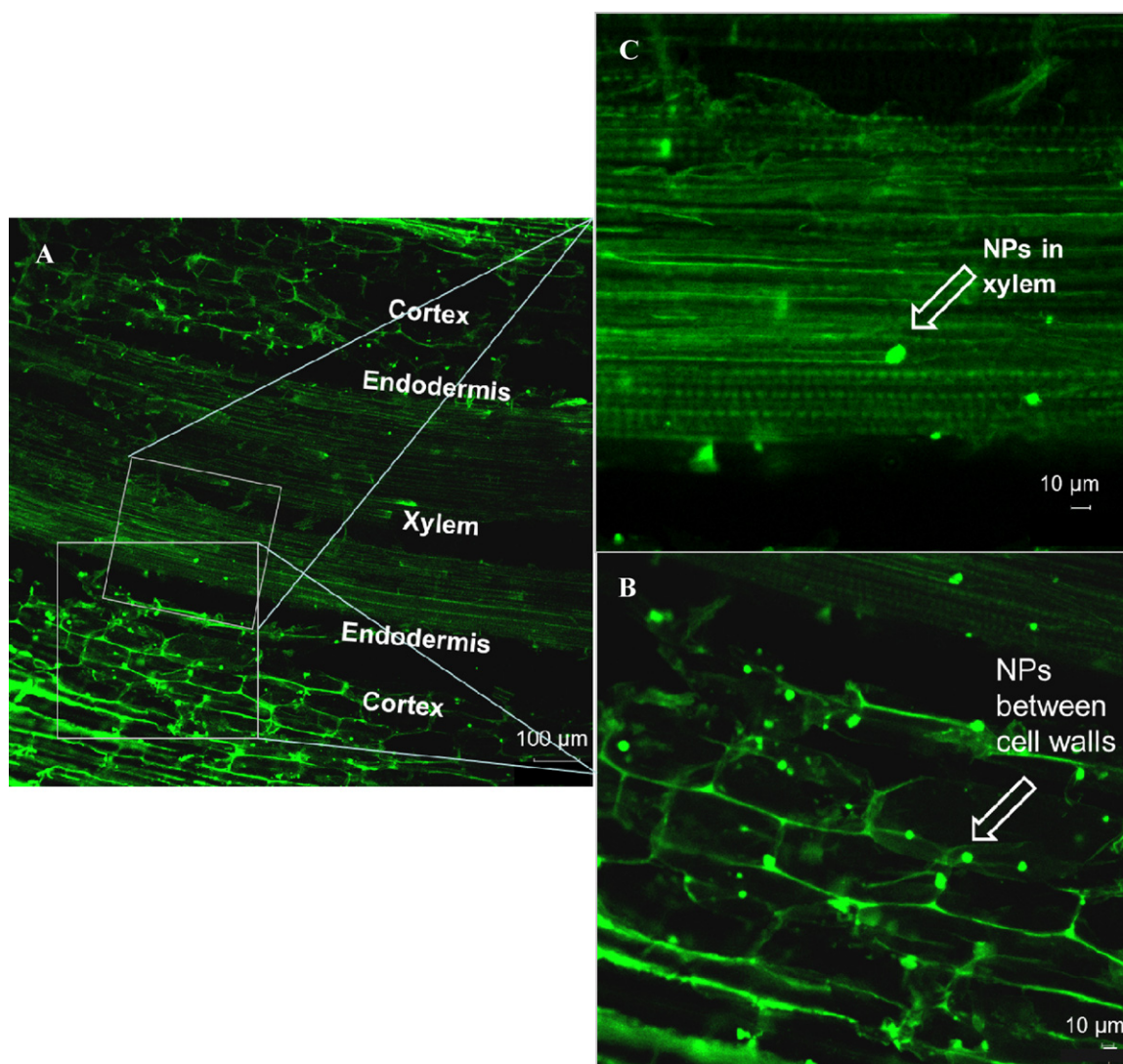


Fig. 4. (A) Confocal image of a longitudinal section of corn root treated for 24 h with 200 mg L^{-1} of FITC-labeled CeO_2 NPs. (B) NP aggregates distributed through cell walls in cortex. (C) NP aggregates within xylem cells. Insets B and C at right are magnifications of the area delimited by the squares in image A.

treated with bare NPs and grown in unenriched soil varied from ~ 0.1 – 0.4 , while in organic soil was below 0.05 . Thus, the soil type plays an important role on the uptake and translocation of NP aggregates.

As seen in Fig. 3, in all cases (uncoated and coated NPs) the concentration of Ce in shoots of plants grown in organic soil was lower compared to unenriched soil. In the case of uncoated NPs, the shoots of corn plants grown in unenriched soil and treated with 100 , 200 , 400 , and $800 \text{ mg CeO}_2 \text{ NPs kg}^{-1}$ had 600 , 236 , 118 , and 168% , respectively more Ce compared to shoots of plants from organic soil. In all cases the differences were statistically significant ($p < 0.05$). In the case of coated NPs (Fig. 3B), the shoots of plants grown in unenriched soil and treated with 200 , 400 and $800 \text{ mg CeO}_2 \text{ NPs kg}^{-1}$ had 104 , 106 and 42% , respectively more Ce compared to plants grown in organic soil. Combining the root results, it can be inferred that organic matter can absorb much amount of NPs on the root surface and hinder their translocation into epidermis. The humic acid is a complex mixture of many acids containing carboxyl and phenolate groups. These functional negatively charged macromolecules attract positive particles that are attached to the root surface. However, these particles do not reach the transport system of the plant; thus, they are not moved to the aboveground plant parts.

3.4. Uptake pathway of CeO_2 NP aggregates by corn plants

Although root tissues have autofluorescence, the images of root and root labeled with FITC were compared using a fluorescence microscope. By using image J software, the root autofluorescence intensity level was found much lower than the FITC fluorescence intensity level in the range of 510 – 550 nm bandpass filter, so the interference coming from root autofluorescence could be neglected (Fig. S3). Fig. S4 shows confocal images of FITC treated roots and FITC-stained CeO_2 NPs treated roots. The root exposed under only FITC exhibit homogeneous fluorescence intensity. As can be seen in Fig. S4B, FITC-stained CeO_2 NPs aggregates can be seen within rooting tissue, from epidermis, endodermis, cortex, and xylem. The presence of stained NP aggregates around vascular vessels, suggests that the NP aggregates found their way to the transport system and moved through the xylem driven by transpiration. This corroborates the presence of Ce in the digested shoot tissues. Previous studies using confocal microscopy have shown that polymeric NPs can penetrate lung cells [36] and CeO_2 NPs can penetrate human bronchial cells [24]; however, these types of cells do not have cell walls. Al-Salim et al. [37] used fluorescence to study the uptake of quantum dots (QD) by walled cell in plants. They observed the fluorescence emission of QD in the vasculature of cut stems of *Allium*

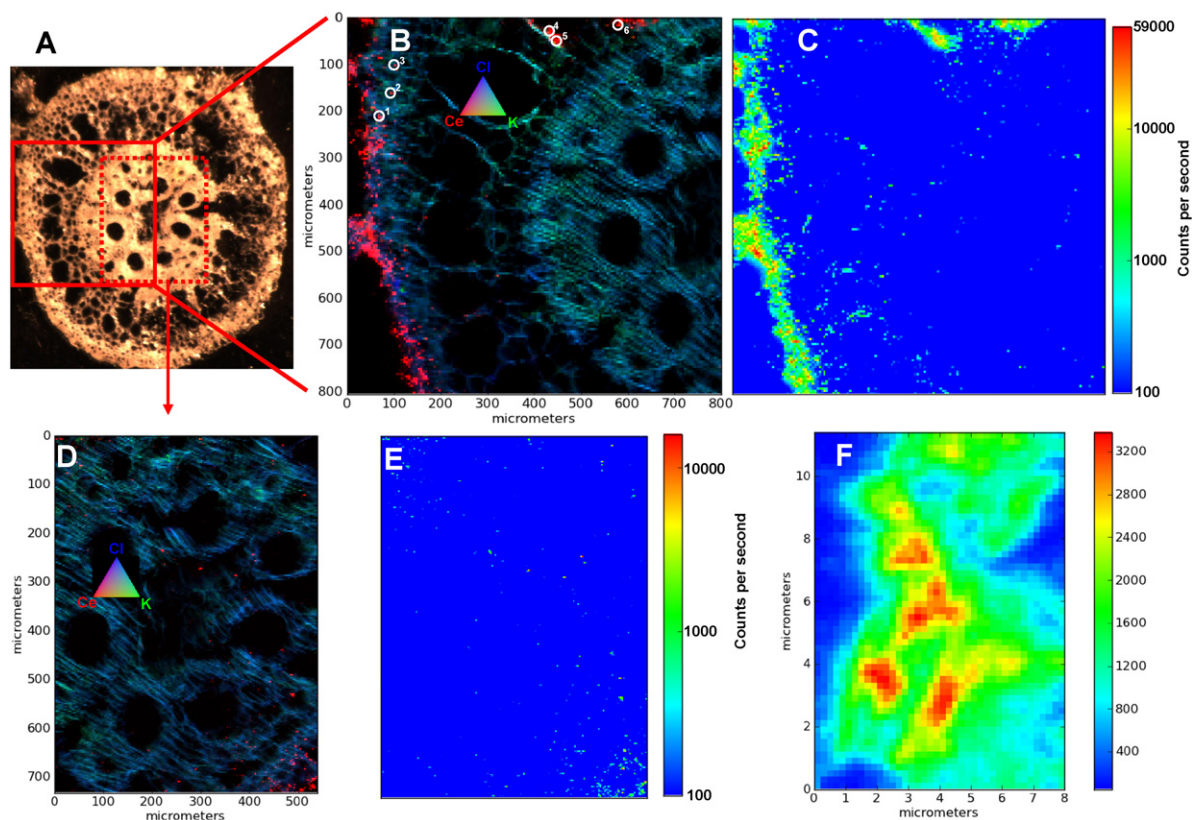


Fig. 5. μ XRF maps of a corn root cross section exposed to CeO_2 NPs. (A) optical image, (B) μ XRF tricolor map epidermis+vascular region, (C) temperature map epidermis+vascular region of the Ce-L^{III} fluorescence line, (D) μ XRF tricolor map vascular region, (E) temperature map vascular region of the Ce-L^{III} fluorescence line, (F) temperature map of Ce particles with 0.2 μm pixel size (maximum resolution). Maps acquired at 5.8 keV with a $0.2 \times 0.8 \mu\text{m}^2$ focused beam and $3 \mu\text{m}^2$ pixel size (except map F).

cepa, *Chrysanthemum* sp., and *Lolium perenne*, but not in the rooted plants [37]. In the present study, FITC-stained CeO_2 NP aggregates were effectively seen within corn plants. Since the NPs can be taken up by roots, another question was raised; how the NP aggregates were transported from epidermis to stele? It is known that apoplastic (through cell wall) and symplastic (through cytoplasm) pathways are main routes to transport. The analysis of longitudinal sections of roots (Fig. 4A) showed the presence of NP aggregates mostly in cell walls of cortex tissues (Fig. 4B) and a few of them into xylem (Fig. 4C). This suggests CeO_2 NP aggregates moved between

cell to cell from epidermis to endodermis by the apoplastic pathway. This explains the low translocation rate from roots to shoots in corn plants. A schematic representation of this behavior is shown in Fig. S5.

3.5. Micro XRF and μ XANES data analyses

The localization and speciation of Ce in the root tissues of corn plants was studied by μ XRF and μ XANES. Fig. 5 shows the micrograph of corn root (A), the μ XRF image (B and D) and the

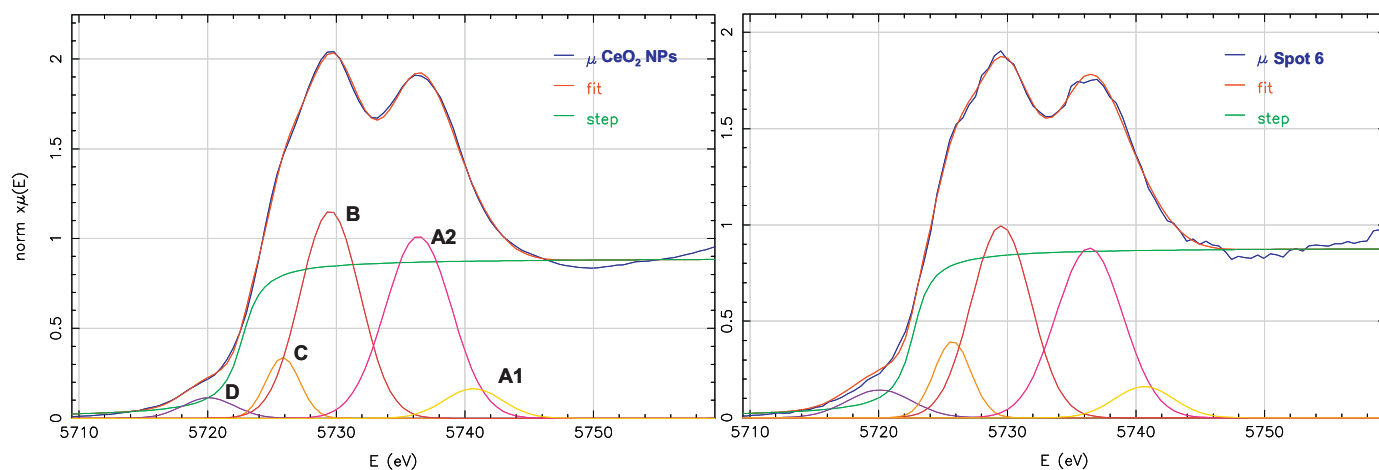


Fig. 6. Example of peak fitting for CeO_2 NPs and μ XANES spot 6 from the corn root. Peaks A1 and A2 correspond to the crystal field split of the $2p_{3/2}5d^*$ final state and Peak B corresponds to a core-excited configuration $2p_{3/2}5d^*L$ (2p denotes the hole in the 2p shell, and $5d^*$ refers to the excited electron in the 5d state, L stands for a hole in the anion ligand). Peak C is due to a combination of crystal field splitting and excitation of different amounts of Ce(III) present in the samples. The pre-edge peak D is the result of a dipole-forbidden $2p_{3/2} \rightarrow 4f$ transition.

Temperature map of epidermis + vascular region of the Ce-L^{III} fluorescence line (C-F). As seen in Fig. 5, Ce intensity is higher in the epidermis of the roots reaching a net intensity of 59,000 cps (Fig. 5B and C). However, Ce signal of lower intensity can be also observed in the central cylinder of the corn roots (Fig. 5D and E). This is in agreement with the results from the confocal microscopy studies performed with FITC labeled CeO₂ NPs (Fig. 4) and reveals the presence of Ce in the vascular region. Synchrotron XRF is unique for studying plant uptake of NPs when coupled to μ XANES. From μ XANES spectra of the Ce L^{III} edge it is possible to obtain information about the chemical species of Ce in the corn root tissues. The spectra obtained from 6 spots in the root sample (3 from the epidermis region and 3 from the cortex region) are very similar to the CeO₂ NPs spectrum (Fig. 6). All the samples analyzed (references and samples) show a spectral signature where Ce is mainly present as Ce(IV). The double whiteline feature with a separation of approximately 7 eV is clear evidence of Ce(IV) oxidation state and corresponds to the core-excited configurations $2p4f05d^*$ and $2p4f15d^*L$, peaks A (sub peaks A1 and A2) and B respectively in Fig. 6 ($2p$ denotes the hole in the $2p$ shell, and $5d^*$ refers to the excited electron in the $5d$ state, L stands for a hole in the anion ligand) [3]. However, slight differences can be found in the spectra which revealed a reduced fraction of Ce and a change in the degree of order of CeO₂. These results have shown that Ce is mainly present as CeO₂ inside the corn root tissues (see Fig. S6).

4. Conclusion

In this research we investigated the behavior of bare and alginate coated CeO₂ NPs in soil and their uptake by corn plants. Results showed that soil organic matter plays an important role in the mobility and bioavailability of CeO₂ NPs in soil solution. Results also showed that organic matter increased the concentration of Ce in roots, especially at high NP treatments (400, 800 mg CeO₂ NPs kg⁻¹ soil). However, the ICP-OES data showed that Ce concentration in shoots was lower in organic matter enriched soil. Surface coating altered the behavior of CeO₂ NPs in both soils and plants. Although the effects of surface coating upon the CeO₂ NPs depend on soil type and organic matter content, alginate surface coating increased the uptake of Ce in CeO₂ NP treated plants. The FITC staining allowed the observation of CeO₂ NPs in cell walls of cortex suggesting passive uptake of these NPs. Moreover, FITC-stained NPs were observed in the vascular cylinder of corn roots, demonstrating that CeO₂ NPs can be taken up by plants. The results suggest that CeO₂ NPs could be introduced into the food chain, threatening environmental and human health.

Acknowledgments

This material is based upon work supported by the National Science Foundation and the Environmental Protection Agency under Cooperative Agreement Number DBI-0830117. Any opinions, findings, and conclusions or recommendations expressed in this material are those of the author(s) and do not necessarily reflect the views of the National Science Foundation or the Environmental Protection Agency. This work has not been subjected to EPA review and no official endorsement should be inferred. The authors also acknowledge the European Synchrotron Radiation Facility, beamline ID21 (ESRF, Grenoble France), the USDA grant numbers 2008-38422-19138 and 2011-38422-30835, the Toxicology Unit of the BBRC (NIH NCRR Grant # 2G12RR008124-16A1), and the NSF Grant # CHE-0840525. Also, the authors thank the staff of the Cell Culture and High Throughput Screening (HTS) Core Facility of UTEP for services and facilities provided. This core facility is supported by grant 5G12RR008124 to the Border Biomedical

Research Center (BBRC), granted to the University of Texas at El Paso from the National Center for Research Resources (NCRR) of the NIH. J.L. Gardea-Torresdey acknowledges the Dudley family for the Endowed Research Professorship in Chemistry.

Appendix A. Supplementary data

Supplementary data associated with this article can be found, in the online version, at <http://dx.doi.org/10.1016/j.jhazmat.2012.05.008>.

References

- [1] V.D. Kosynkin, A.A. Arzgatkina, E.N. Ivanov, M.G. Chtoutsu, A.I. Grabko, A.V. Kardapolov, N.A. Sysina, The study of process production of polishing powder based on cerium dioxide, *J. Alloys Compd.* 303–304 (2000) 303–304.
- [2] A. Corma, P. Atienzar, H. Garcia, J.-Y. Chane-Ching, Hierarchically mesostructured doped CeO₂ with potential form solar-cell use, *Nat. Mater.* 3 (2004) 394–397.
- [3] F.E. Livingston, H. Helvajian, Variable UV laser exposure processing of photo-sensitive glass-ceramics: maskless micro to meso-scale structure fabrication, *Appl. Phys. A: Mater. Sci. Proc.* 81 (2005) 1569–1581.
- [4] K. Van Hoecke, J.T.K. Quick, J. Mankiewicz-Boczek, A. De Schampelaere, P. Van der Meeren, C. Barnes, G. McKerr, C. Vyvyan Howard, D. Van De Meent, K. Rydzynski, K.A. Dawson, A. Salvati, A. Lesniak, I. Lynch, G. Silversmit, B. De Samber, L. Vincze, C.R. Janssen, Fate and effects of CeO₂ nanoparticles in aquatic ecotoxicity tests, *Environ. Sci. Technol.* 43 (2009) 4537–4546.
- [5] L.K. Limbach, R. Bereiter, E. Muller, R. Krebs, R. Galli, W.J. Stark, Removal of oxide nanoparticles in a model wastewater treatment plant: influence of agglomeration and surfactants on clearing efficiency, *Environ. Sci. Technol.* 42 (2008) 5828–5833.
- [6] Z. Li, E. Sahle-Demessie, A.A. Hassan, G.A. Sorial, Transport and deposition of CeO₂ nanoparticles in water-saturated porous media, *Water Res.* 45 (2011) 4409–4418.
- [7] G. Cornelis, B. Ryan, M.J. McLaughlin, J.K. Kirby, D. Beak, D. Chittleborough, Solubility and batch retention of CeO₂ nanoparticles in soils, *Environ. Sci. Technol.* 45 (2011) 2777–2782.
- [8] A. Thill, O. Zeyons, O. Spalla, F. Chauvat, J. Rose, M. Auffan, A.M. Flank, Cytotoxicity of CeO₂ nanoparticles for *Escherichia coli*. Physico-chemical insight of the cytotoxicity mechanism, *Sci. Total Environ.* 40 (2006) 6151–6156.
- [9] B.D. Johnston, T.M. Scown, J. Moger, S.A. Cumberland, M. Baalousha, K. Linge, R. van Aerle, K. Jarvis, J.R. Lead, C.R. Tyler, Bioavailability of nanoscale metal oxides TiO₂, CeO₂, and ZnO to fish, *Sci. Total Environ.* 44 (2010) 1144–1151.
- [10] L.K. Limbach, Y. Li, R.N. Grass, T.J. Brunner, M.A. Hintermann, M. Muller, D. Gunther, W.J. Stark, Oxide nanoparticle uptake in human lung fibroblasts: effects of particle size, agglomeration, and diffusion at low concentrations, *Sci. Total Environ.* 39 (2005) 9370–9376.
- [11] W. Lin, Y. Huang, X. Zhou, Y. Ma, Toxicity of cerium oxide nanoparticles in human lung cancer cells, *Int. J. Toxicol.* 25 (2006) 451–457.
- [12] M.L. Lopez-Moreno, G. de la Rosa, J.A. Hernandez-Viezcas, J.R. Peralta-Videa, J.L. Gardea-Torresdey, X-ray absorption spectroscopy (XAS) corroboration of the uptake and storage of CeO₂ nanoparticles and assessment of their differential toxicity in four edible plant species, *J. Agric. Food Chem.* 58 (2010) 3689–3693.
- [13] M.L. Lopez-Moreno, G. de la Rosa, J.A. Hernandez-Viezcas, H. Castillo-Michel, C.E. Botez, J.R. Peralta-Videa, J.L. Gardea-Torresdey, Evidence of the differential biotransformation and genotoxicity of ZnO and CeO₂ nanoparticles on soybean (*Glycine max*) plants, *Environ. Sci. Technol.* 44 (2010) 7315–7320.
- [14] K. Birbaum, R. Brogioli, M. Schellenberg, E. Martinoia, W.J. Stark, D. Günther, L.K. Limbach, No evidence for cerium dioxide nanoparticle translocation in maize plants, *Environ. Sci. Technol.* 44 (2010) 8718–8723.
- [15] K. Dietz, S. Herth, Plant nanotoxicology, *Cell* 16 (2011) 582–589.
- [16] X. Ma, J. Geiser-Lee, Y. Deng, A. Kolmakov, Interactions between engineered nanoparticles (ENPs) and plants: phytotoxicity, uptake and accumulation, *Sci. Total Environ.* 408 (2010) 3053–3061.
- [17] C.M. Rico, S. Majumdar, M. Duarte-Gardea, J.R. Peralta-Videa, J.L. Gardea-Torresdey, Interaction of nanoparticles with edible plants and their possible implications in the food chain, *J. Agric. Food Chem.* 59 (2011) 3485–3498.
- [18] M.M. Goodman, Maize, in: N.W. Simmonds (Ed.), *Evolution of Crop Plants*, Longman, New York, 1979, pp. 128–136.
- [19] S.J. Klaine, P.J.J. Alvarez, G.E. Batley, T.F. Fernandes, R.D. Handy, D.Y. Lyon, S. Mahendra, M.J. McLaughlin, J.R. Lead, Nanomaterials in the environment: behavior, fate, bioavailability, and effects, *Environ. Toxicol. Chem.* 27 (2008) 1825–1851.
- [20] J.G. Parsons, M.L. Lopez, C. Gonzalez, J.R. Peralta-Videa, J.L. Gardea-Torresdey, Toxicity and biotransformation of uncoated and coated nickel hydroxide nanoparticles on mesquite plants, *Environ. Toxicol. Chem.* 29 (2010) 1146–1154.
- [21] D. Lin, B. Xing, Root uptake and phytotoxicity of ZnO nanoparticles, *Environ. Sci. Technol.* 42 (2008) 5580–5585.
- [22] Z. Cifuentes, L. Custardoy, J.M. Fuente, M.R. Ibarra, D. Rubiales, A. Luque, Absorption and translocation to the aerial part of magnetic carbon-coated

- nanoparticles through the root of different crop plants, *J. Nanobiotechnol.* 8 (2010) 1–8.
- [23] E. Wild, K.C. Jones, Novel method for the direct visualization of in vivo nano-materials and chemical interactions in plants, *Environ. Sci. Technol.* 43 (2009) 5290–5294.
- [24] T. Xia, M. Kovochich, M. Liong, L. Madler, B. Gilbert, H. Shi, J.I. Yeh, J.I. Zink, A.E. Nel, Comparison of the mechanism of toxicity of zinc oxide and cerium oxide nanoparticles based on dissolution and oxidative stress properties, *ACS Nano* 2 (2008) 2121–2134.
- [25] Q. Liu, B. Chen, Q. Wang, X. Shi, Z. Xiao, J. Lin, X. Fang, Carbon nanotubes as molecular transporters for walled plant cells, *Nano Lett.* 9 (2009) 1007–1010.
- [26] A.A. Keller, H. Wang, D. Zhou, H.S. Lenihan, G. Cherr, B.J. Cardinale, R. Miller, Z. Ji, Stability and aggregation of metal oxide nanoparticles in natural aqueous media, *Environ. Sci. Technol.* 344 (2010) 1962–1967.
- [27] G.S.R. Krishnamurti, R. Naidu, Solid-solution speciation and phytoavailability of copper and zinc in soils, *Environ. Sci. Technol.* 36 (2002) 2645–2651.
- [28] J. Susini, M. Salomé, U. Neuhaeusler, O. Dhez, D. Eichert, B. Fayard, A. Somogyi, S. Bohic, P. Bleuet, G. Martinez-Criado, R. Tucoulou, A. Simionovici, M. Barrett, R. Drakopoulos, The X-ray microscopy and micro-spectroscopy facility at the ESRF, *Synchrotron Radiat. News* 16 (2003) 35–43.
- [29] V.A. Solé, E. Papillon, M. Cotte, P. Walter, J. Susini, A multiplatform code for the analysis of energy-dispersive X-ray fluorescence spectra, *Spectrochim. Acta Part B* 62 (2007) 63–68.
- [30] P. Nachimuthu, W. Shih, R. Liu, L. Jang, J. Chen, The study of nanocrystalline cerium oxide by X-ray absorption spectroscopy, *J. Solid State Chem.* 149 (2000) 408–413.
- [31] K. Yang, D. Lin, B. Xing, Interaction of humic acid with nanosized inorganic oxides, *Langmuir* 25 (2009) 3571–3576.
- [32] A. Hajdu, E. Elles, E. Tombacz, I. Borbath, Surface charging, polyanionic coating and colloid stability of magnetite nanoparticles, *Colloids Surf. A: Physicochem. Eng. Aspects* 347 (2009) 104–108.
- [33] T. Hiemstra, J. Antelo, A.M.D. van Rotterdam, W.H. van Riemsdijk, Nanoparticles in natural systems II: the natural oxide fraction at interaction with natural organic matter and phosphate, *Geochim. Cosmochim. Acta* 74 (2010) 59–69.
- [34] D.A. Navarro, M.A. Bisson, D.S. Aga, Investigating uptake of water-dispersible CdSe/ZnS quantum dot nanoparticles by *Arabidopsis thaliana*, *J. Hazard. Mater.* 211–212 (2012) 427–435.
- [35] J. Douch, M. Hamdani, H. Fessi, A. Elaissari, Acid-base behavior of a colloidal clays fraction extracted from natural quartz sand: effect of permanent surface charge, *Colloids Surf. A: Physicochem. Eng. Aspects* 338 (2009) 51–60.
- [36] A. Salvati, C. Alberg, S. dos Santos, J. Varela, P. Pinto, I. Lynch, K.A. Dawson, Experimental and theoretical comparison of intracellular import of polymeric nanoparticles and small molecules: toward models of uptake kinetics, *Nanomedicine* 7 (2011) 818–826.
- [37] N. Al-Salim, E. Barraclough, E. Burgess, B. Clothier, M. Deurer, S. Green, L. Malone, G. Weir, Quantum dot transport in soil, plants, and insects, *Sci. Total Environ.* 409 (2011) 3237–3248.